*CHARGE AND WAVELENGTH SCALING OF RF PHOTOINJECTORS: A DESIGN TOOL**

J. Rosenzweig and E. Colby
UCLA Department of Physics and Astronomy, Los Angeles, CA 90024, USA

The optimum design of an emittance compensated rf photoinjector is very complicated and time-consuming, relying heavily on multi-particle simulations without good analytical models as a guide. Emittance compensated designs which have been developed, however, can be used to generate other designs with no additional effort if the original design is scaled correctly. This paper examines the scaling of rf photoinjector design with respect to charge and wavelength, and presents emittance and brightness scaling laws for these variables. Parametric simulation studies are presented to illustrate these scaling laws. A practical design for the TESLA FEL rf photo-injector is developed using these scaling techiniques.

I. INTRODUCTION

The optimization of an rf photoinjector[1-6] design is typically an iterative and somewhat haphazard process. This is because, while some scaling laws concerning photoinjector performance have been derived from first order integration of the transverse force equations [2], an optimized photoinjector will necessarily use emittance compensation [3], which is a dynamical process with only a qualitative theoretical understanding. A full design requires a search of the relevant parameter space, which includes the rf amplitudes of the gun and linac, the focusing lens position and strength, the gun-to-linac separation, the cathode cell length, and the beam charge, spot size and pulse length. Because this is such an involved process, including detailed rf and magnet design calculations and multiparticle simulations, any analytical understanding of the optimization process would be a useful and time-saving tool. While a full analytical theory of the beam dynamics in an rf photoinjector remains a difficult result [7], this work presents a new method, that of scaling an existing rf optimized photoinjector design with respect to charge and wavelength variation to design entire families of optimized photoinjectors.

II. DYNAMICS EQUATIONS

The longitudinal and transverse dynamics of the electrons in an rf photoinjector can be described by some relatively straightforward equations. Since the longitudinal motion is dominated by the applied rf fields, and the collective effects due to the electrons are perturbations on the motion of a single electron, for this discussion it is sufficient to examine the single particle dynamics. The rf acceleration field in a pure π-mode standing wave accelerator gives energy gain equation [2]

$$\frac{d\gamma}{dz} = \frac{eE_0}{2m_e c^2}\left[\sin(\phi) + \sin(\phi + 2k_z z)\right], \qquad (1)$$

where $k_z = \omega/c$ is the rf wave number, and E_0 is the peak acceleration field. The evolution of phase angle $\phi = k_z z - \omega t + \phi_0$ (relative to the forward wave) is

$$\frac{d\phi}{dz} = k_z\left(1-\beta^{-1}\right) = k_z\left[1 - \frac{\gamma}{\sqrt{\gamma^2 - 1}}\right]. \qquad (2)$$

By recasting the equations using the dimensionless independent variable $\tilde{z} \equiv k_z z$,

$$\frac{d\gamma}{d\tilde{z}} = \alpha\left[\sin(\phi) + \sin(\phi + 2k_z z)\right] \qquad (3)$$

$$\text{and} \quad \frac{d\phi}{d\tilde{z}} = \left[1 - \frac{\gamma}{\sqrt{\gamma^2 - 1}}\right], \qquad (4)$$

where $\alpha \equiv eE_0/2k_z m_e c^2$ is the single parameter[2] which describes the longitudinal motion. This immediately gives the result that the scaling of an rf design with wavelength implies that α must be kept constant as the wavelength is varied.

The transverse dynamics of an optimized rf photoinjector are a bit more intricate to describe, because the collective forces due to space-charge are non-negligible throughout the device. In fact, the uncorrelated thermal motion of the beam particles is nearly ignorable in optimized rf photoinjectors because of the dominance of space charge and externally applied forces. This situation allows a key simplification in modeling the collective transverse dynamics, that the motion can be assumed to be nearly laminar and an ordering of particles in the spatial coordinates is preserved in this case.

Given this situation, assuming the configuration space distribution functions of the beam at the cathode are the scaled correctly, the scaling of the transverse motion of the electron distribution can be deduced by examining the scaling of the rms transverse envelope equations. For this work, we write the envelope equation describing the evolution of a cylindrically symmetric beam, igoring thermal emittance effects [7],

$$\sigma_x'' + \sigma_x'\left(\frac{(\beta\gamma)'}{\beta\gamma}\right) + K_x\sigma_x = \frac{2I}{I_0(\beta\gamma)^3\sigma_x} f\left(\frac{\sigma_x}{\beta\gamma\sigma_z}\right), \qquad (5)$$

* *Work supported by U.S. DOE grants DE-FG03-90ER40796 and DE-FG03-92ER40693, and Sloan Foundation grant BR-3225.*

where an analogous equation exists for σ_y. In Eq. 5 the prime indicates the derivative with respect to z, the focusing strength (which is the square of a betatron wave number) $K_x \equiv k_\beta^2 = -F_{\text{ext}}/\beta^2\gamma m_e c^2 x$ for all linear static externally applied forces, I is the peak current, and $I_0 \approx 17$ kA.

III. CHARGE SCALING

Often, one designs an rf photoinjector with a particular application in mind, specifying the charge Q, bunch length σ_z, and total (including nonthermal sources) emit-tance ε, only to find another significantly different application arising later. An rf photoinjector design can be scaled quite straightforwardly by scaling the defocusing forces of the bunch appropriately. This can be seen by writing $I = Qc/g\sigma_z$, where g is a distribution function dependent form factor, and using the defocusing space charge term in Eq. 5 to define the rms defocusing (imaginary) wave number as

$$\kappa_{sc}^2 = \frac{2I}{I_0(\beta\gamma)^3\sigma_r^2} f\left(\frac{\sigma_x}{\beta\gamma\sigma_z}\right) = \left[\frac{2c}{I_0\beta^2\gamma^3}\right]\left[\frac{Q}{g\sigma_z\sigma_x^2}\right] f\left(\frac{\sigma_x}{\beta\gamma\sigma_z}\right) \quad (6)$$

The first bracketed factor in Eq. 6 is a bunch independent constant, the second is, up to a distribution shape dependent constant, the peak beam density, and the last factor is dependent only on the bunch aspect ratio. Therefore one can scale a design keeping all of the applied focusing forces the same by preserving the defocusing space charge wave number, which implies that peak the beam density, aspect ratio and distribution shape must be kept constant. Quantitatively we can write this as a simple scaling law,

$$\sigma_i \propto Q^{1/3}, \quad (7)$$

all bunch dimensions scale as the cube-root of the total charge.

To check on how well this scaling works in actual practice, a series of simulations were performed using the code PARMELA, which includes all applied fields and an electrostatic approximation to the self-consistent space charge fields. A test injector composed of a high gradient 1-1/2 cell S-band (2856 MHz) photoinjector gun with BNL-style cavity profiles [4], followed by a focusing solenoid, and a drift long enough to allow the compensation minimum to be clearly discerned was chosen for the scaling studies.

The results of these studies are discussed in detail in Ref. 8, and are summarized here. The evolution of the beam prof-iles for various charge beams is essentially of the same form. In addition, the evolution of the rms normalized emittance displays qualitatively similar behavior. It is then reasonable to ask how the emittance quantitatively scales following this prescription for Q scaling. This is not a trivial task, as there are a number of contributions to the normalized rms emittance, defined by

$$\varepsilon_x = (m_e c)^{-1}\sqrt{\langle x^2\rangle\langle p_x^2\rangle - \langle xp_x\rangle}. \quad (8)$$

To begin, we examine the dependence of the space-charge derived emittance. All of the force integrals needed to find the rms transverse momentum scale (including the nonlinear com-ponents of the force, but not including the cathode effects) as the beam size, and the space-charge derived emittance scales as

$$\varepsilon_x^{sc} \propto \sigma_x^2 \propto Q^{2/3} \quad (9)$$

This is the same dependence that Kim[2] has deduced for the uncompensated space charge emittance.

Another source of rms emittance is the differential focusing (as a function of longitudinal position) due to the linear transverse rf forces. This effect has been analyzed to lowest order by Kim[2], who found

$$\varepsilon_x^{rf} \approx \left(\frac{eE_0}{\sqrt{8}m_e c^2}\right)(k_z\sigma_z)^2\sigma_x^2 \propto Q^{4/3}. \quad (10)$$

The emittance again scales as the square of the transverse beam size, and additionally scales as the length of the beam squared.

A final contribution to the total rms emittance arises because of the beam's energy spread. Since this quantity increases as the square of the beam length, the possible emittance growth due to chromatic aberrations in the focusing system will increase with bunch charge. This effect scales as

$$\varepsilon_x^{ch} \propto \left(\frac{\Delta p}{p}\right)\left(\frac{\sigma_x^2}{f}\right) \propto (k_z\sigma_z)^2\sigma_x^2 \propto Q^{4/3}. \quad (11)$$

The chromatic effects have the same scaling as linear rf emittance contribution.

Simulation results of all of the Q scaled designs is shown in Fig. 1. The asymptotic predictions of the emittance growth, that it should be space-charge dominated at low charge ($\varepsilon_x \propto Q^{2/3}$) and rf/chromatic dominated ($\varepsilon_x \propto Q^{4/3}$) at high charge are shown, as is a simple fit to a curve which is the sum of squares of these two asymptotic effects ($\varepsilon_x = \sqrt{\left(aQ^{2/3}\right)^2 + \left(bQ^{4/3}\right)^2}$). Note that for a large range of charges, the dependence of emittance on charge is in the transition between the two limits, and is approximately linear.

IV. WAVELENGTH SCALING

Another situation which can arise is that one laboratory develops a sophisticated rf photoinjector design at a certain rf wavelength, and a different laboratory wishes to take advantage of this work in adapting the design to another, more convenient wavelength. This naturally brings up the question of wavelength (λ) scaling of photoinjector design.

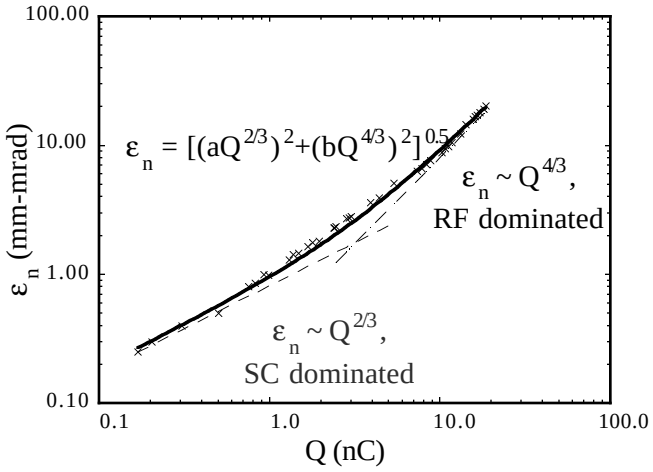

Figure 1. PARMELA simulation of emittance compensated BNL-style gun, emittance dependence of charge scaling.

This discussion proceeds immediately from Eqs. 3 and 4, which dictate the scaling of the electric field, as mentioned before. To preserve the longitudinal motion in a design - the injection phasing, compression of longitudinal phase spread, the energies at the exit of the rf structures, etc. - one must simply follow the scaling $E_0 \propto \lambda^{-1}$. This implies that the structure length is simply proportional to the rf wavelength. Further, preservation of the relative energy spread requires that the beam's injected phase spread be constant, $\sigma_z \propto \lambda$.

For preservation of the transverse dynamics, one must scale all of the transverse wave numbers inversely with the rf wavelength, since all distances must scale with wavelength. For solenoidal focusing, this implies $B \propto \lambda^{-1}$. It can be shown that the transverse rf effects naturally scale correctly with wavelength if the field is inversely proportional to the wavelength [8]. For space charge, we recall that the aspect ratio of the beam must remain constant when scaling, and thus we have $\sigma_{x,y} \propto \lambda$. To scale the space charge defocusing wave number correctly, we deduce from Eq. 6 that $Q \propto \lambda$.

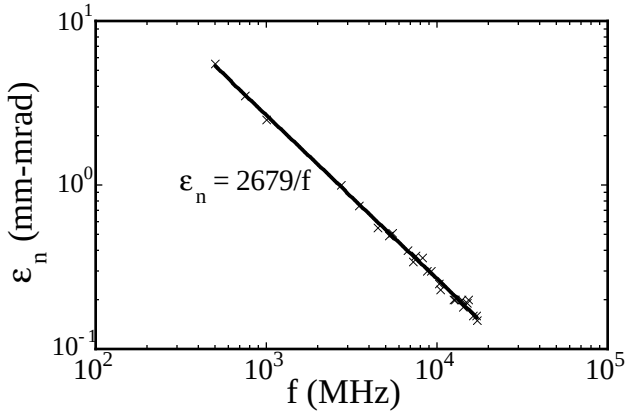

Figure 2. PARMELA simulation of emittance compensated BNL-style gun, emittance dependence of wavelength scaling.

These scaling rules have also been tested with PARMELA simulations, as described in Ref. 8. The evolution of the beam size along the beamline, with all lengths normalized to the rf wavelength, are invariant in these simulations. In addition, the emittance evolution in displayed identical scaling behavior. To see why this is so, we note that for λ scaling, the rms momentum integrals are proportional to the defocusing strength ($\sim \lambda^{-2}$), the beam size ($\sim \lambda$) the total rest frame integration time ($\sim \lambda$). Multiplied by the rms beam size ($\sim \lambda$), we find that $\varepsilon_x^{sc} \propto \lambda$. The rf contribution to the emittance scales with wavelength, using Eq. 10, as $\varepsilon_x^{rf} \propto E_0 (k_z \sigma_z) \sigma_x' \propto \lambda$. Finally, the contribution to the emittance from chromatic aberrations scales, using Eq. 11, as $\varepsilon_x^{cr} \propto (\Delta p/p)(\sigma_x^c / f) \propto f^{-1} (k_z \sigma_z)^{-} \sigma_x^c \propto \lambda$. These results, which lead to the conclusion that the emittance is yet another "length" simply proportional to λ, is easily shown to be valid by the numerical simulations, as seen in Fig. 2.

V. SCALING: A DESIGN EXAMPLE

A short wavelength FEL has been proposed for The TESLA Test Facility (TTF) [9]. While a 1.3GHz BNL-style photoinjector has been designed for the TTF [10], its focusing scheme has been optimized to produce high charge (8.3 nC) bunches. When charge scaling is applied to reduce the charge to the FEL design-driven 1 nC, one does not obtain an emittance below 2 mm-mrad. On the other hand, if one scales the BNL 1 nC design (with its focusing scheme) first to 1.3 GHz (so the charge is 2.2 nC) and then scales the charge back down to 1 nC, the BNL focusing scheme produces much better emittances, well below the 1 mm-mrad demanded by the FEL fter acceleration in a booster linac. This excellent example of the use of scaling in design is shown in Fig. 3.

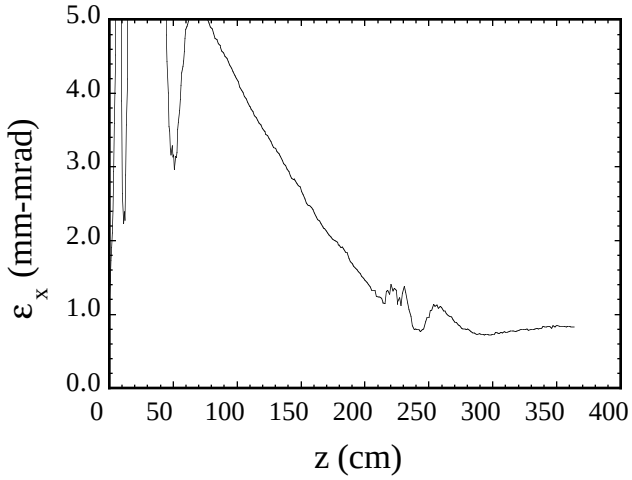

Figure 3. BNL-style design scaled to f=1.3 GHz, and 1 nC. A TESLA cavity (15 MV/m) booster linac at z=240 cm aids and preserves emittance compensation. In the gun E_0=45 MV/m.

VI. REFERENCES

[1] J. Fraser, *et al., IEEE Trans.Nuc.Sc.* **NS-32**,1791 (1985)

[2] K.J.Kim, *Nucl. Instr. Methods A* **275**, 201 (1988).

[3] B.E. Carlsten, Nucl. Instr. and Meth. A 285 (1989) 313.

[4] J.C. Gallardo and H. Kirk, *Proc. Particle 1993 Accel. Conf.* 3615 (IEEE, 1993)

[5] R. Sheffield, *et al., NIM A* **341**, 371 (1994)

[6] L. Serafini, *Nucl. Instr. Methods A* **340**, 40 (1994).

[7] L. Serafini and J. Rosenzweig, these proceedings.

[8] J. Rosenzweig and E. Colby, to be published in Proc. of the 1994 Advanced Accelerator Workshop (AIP, 1995).

[9] J. Rossbach, these proceedings.

[10] E. Colby *et al.*, these proceedings.